Identification of Nucleation Loci in Emulsion Polymerization Processes. II. A Systematic Study of Liquid–Liquid Emulsions

Vineet Shastry,[1] L. H. Garcia-Rubio[2]

[1]*Department of Chemical Engineering, University of South Florida, E. Fowler Avenue, Tampa, Florida 33620*
[2]*College of Marine Sciences, University of South Florida, 140 7th Avenue South, St. Petersburg, Florida 33701*

Received 28 May 2004; accepted 19 January 2005
DOI 10.1002/app.22055
Published online 9 February 2006 in Wiley InterScience (www.interscience.wiley.com).

ABSTRACT Identification of the main nucleation sites and characterizing them in terms of their size and composition is prime objective of this research effort. Different nucleation sites have been proposed as the most likely nucleation sites by various researchers. Recent advances in the development of the spectroscopic techniques enable comprehensive characterization of the emulsion at the beginning of the reaction. In this paper, we present the experimental evidence of the existence of a previously unidentified nano-droplet population of size range 30 to 100 nm in diameter using spectroscopy. Presence of about seventy to eighty percent of the dispersed phase in the nano-droplet population and large interfacial area make them the most probable particle nucleation loci in emulsion polymerization processes. © 2006 Wiley Periodicals, Inc. J Appl Polym Sci 100: 2858–2866, 2006

Key words: emulsion polymerization; particle nucleation; UV-vis spectroscopy

INTRODUCTION

Particle nucleation is the forcing function in emulsion polymerization reactions, and as such, it plays a significant role in the development of the properties of the final latex. The nucleation mechanism for particle formation is not fully understood, and it is a subject of considerable controversy.[1,2] In part I of this work, inferences drawn from theoretical simulations and experimental observations are presented to advance the hypothesis that a likely locus for particle nucleation is a previously unidentified population of nanodroplets ranging in size from 30 to 100 nm. Part II of this work focuses on the description of the experimental efforts used to support the hypothesis proposed in part I and explores some of the experimental conditions known to affect the nanodroplet population.

To identify the locus of particle nucleation, it is necessary to establish the state of the reacting mixture at the time of addition of the initiator (time zero). At this point, the reacting mixture is essentially a liquid–liquid emulsion. In contrast to the techniques reported elsewhere[1,2] in which inferences on the initial conditions are made on the basis of data sampled during polymerization, we propose to characterize the initial conditions of the reaction mixture through the study of liquid–liquid emulsions with ultraviolet–visible (UV–vis) spectroscopy. The experiments reported herein were conducted with nonreacting model systems. The effects of the emulsification conditions on the initial droplet populations were investigated; the results and observations from the experimental investigation are reported and discussed together with theoretical considerations and recommendations for future work.

EXPERIMENTAL

Model system

In the context of this study, a model emulsion system consists of continuous and discrete phases that approximate the dispersion characteristics of the emulsions prepared in the reactors before the beginning of the polymerization reactions. The molecules incorporated in the model system are selected so that they have physicochemical properties similar to those of the monomers but optical properties favorable to the detection of the different particle populations and chromophoric groups present in the mixture. Under similar emulsification conditions (temperature, pH, and surfactant concentration), dispersed phases having similar physicochemical properties (viscosity, sol-

Correspondence to: L. H. Garcia-Rubio (garcia@seas.marine.usf.edu).

Contract grant sponsor: Particle Engineering Research Center at the University of Florida; contract grant number: NSF EEC-94-02989.
Contract grant sponsor: ICI-Glidden.
Contract grant sponsor: Lucent Technologies.
Contract grant sponsor: Xerox.

TABLE I
Comparison of Relevant Physical Properties of Styrene, Butyl Methacrylate, and Decane

Physical property	Styrene	Butyl methacrylate	Decane
Density (g/cm^3)	0.906	0.889	0.73
Vapor pressure (mmHg)	5	4.9	1.4
Interfacial tension (dyn/cm)	27.7	28	30.4
Viscosity (cp)	0.675	0.832	0.863

ubility, and density) display similar dispersion characteristics.[1] Liquid–liquid emulsions of a homolog series of alkanes ranging from C_7 to C_{70} have been investigated to explore the dispersion characteristics of potential model systems,[3] and as can be appreciated in Table I, the dispersion characteristics of decane and its relevant physicochemical properties[4–8] are sufficiently close to those of styrene[4,5,9,10] and butyl methacrylate[4,5,11–13] to provide an adequate reference system. Therefore, decane was used as the oil phase (dispersed phase) in this study. In addition to its physicochemical properties, decane is transparent throughout the UV–vis portion of the spectrum, lending itself to the use of labeled emulsifiers, such as sodium dodecyl benzene sulfonate (SDBS), which has distinct absorption bands between 200 and 300 nm. The optical properties of both decane and SDBS provide a good contrast to the continuous medium [phosphate buffer saline (PBS)] for transmission spectroscopy measurements.

Materials and equipment

PBS, used as the continuous phase, was obtained from Florida Blood Services (St. Petersburg, FL). Spectral-grade decane and SDBS were obtained from Sigma Aldrich (St. Louis, MO). HCl and NaOH were obtained from Fisher Scientific (PA).

The emulsions were prepared in a 500-mL glass reactor. An electric temperature controller was used to adjust the heat of the jacket to maintain a desired constant temperature inside the reactor. Two baffles were added to the reactor to break the vortex due to agitation. The stirrer rod passed through the central opening of the reactor lid. A motor rotated the stirrer, providing constant agitation at 500 rpm. The rate of rotation was verified with a stroboscope for each experiment. A sample slip stream, drawn continuously from the reactor with the help of the sample pump, was sent to the dilution system, in which it was diluted with the suspending medium.[14] The temperature of the diluent was kept the same as that of the emulsion. The flow rates of the diluent stream and the sample slip stream were such that the transmission spectrum of the diluted emulsion always was within

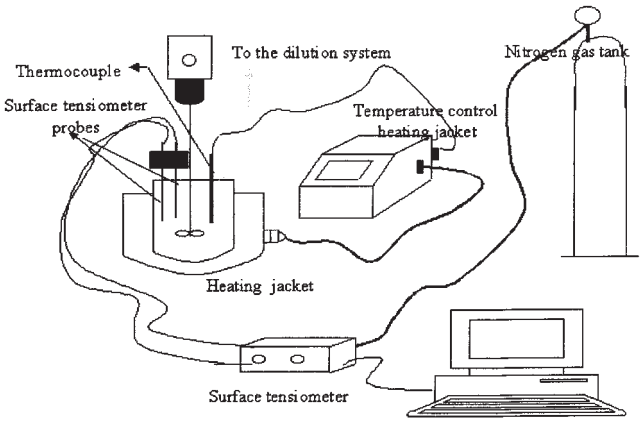

Figure 1 Schematic of the experimental setup for the experiments with model systems.

the linear range of the spectrometer system used to monitor the emulsions continuously. The spectrometer was a Hewlett–Packard HP8452A UV–vis spectrometer (Palo Alto, CA) with a resolution of 2 nm. The sample cell holder of the spectrometer was also maintained at the desired temperature with a model C5700820 electrical temperature controller manufactured by PerkinElmer (Wellesley, MA). All hoses and tubes were insulated with glass fiber to minimize heat losses. The pH of the suspending medium and the diluent was monitored with a Fisher Accumet 610 pH meter. The two surface tensiometer probes, through which nitrogen was bubbled, were placed in the reactor to measure the interfacial tension of the emulsion.[11] Figures 1 and 2 show the schematics of the experimental setup.

Methods

The emulsions were prepared in PBS. The pH of PBS was adjusted with either HCl or NaOH. The emul-

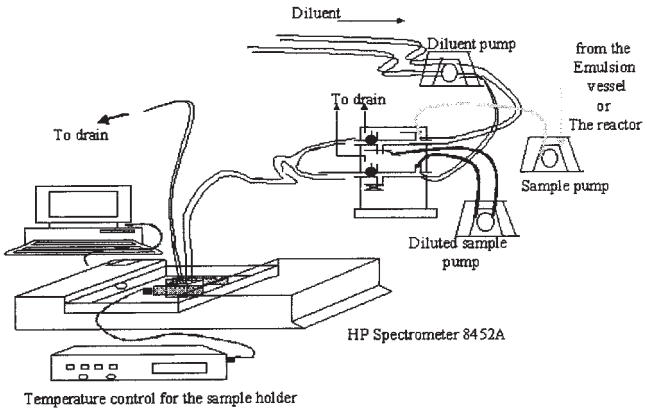

Figure 2 Schematic of the experimental setup including the dilution system for the experiments with model emulsion systems.

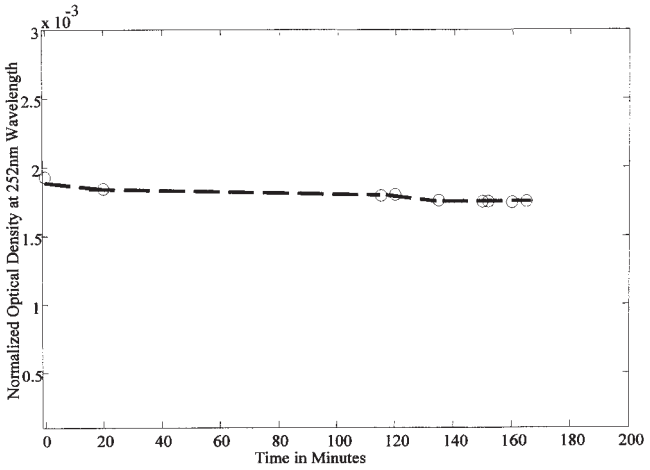

Figure 3 Normalized OD at 252 nm measured as a function of time (OD remains constant after the emulsion has stabilized).

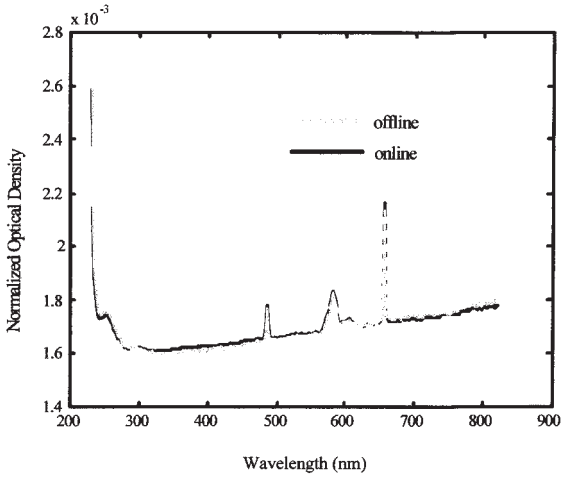

Figure 4 Comparison of typical offline and online normalized OD spectra of a decane-in-PBS emulsion after the emulsion has reached stability (the narrow widths above 450 nm are artifacts due to the lamp emission).

sions were prepared by the addition of 150 mL of the suspending medium to the 500-mL glass reactor placed in the temperature-controlled jacket (Figs. 1 and 2). An additional 30 mL of the appropriate surfactant solution was added to the suspending medium. The surfactant solution was prepared at the concentration dictated by the experimental design (see the Experimental Design section). The contents in the reactor were heated until the desired temperature was reached. At this point, 160 mL of decane was added. The reactor contents were kept under continuous agitation at 500 rpm to form the emulsion. After it was verified that the emulsion was stable, it was sampled for analytical purposes. A sample of the emulsion inside the reactor was pumped into the dilution-measurement system (Fig. 2) with a rotary peristaltic pump. The spectrum of the emulsions was continuously monitored. At the desired time intervals, the spectra were saved for further analysis.

Emulsion stability

To determine the time required to obtain a stable emulsion, experiments were performed at room temperature with the emulsion prepared (see the previous section) at pH 7 and with a surfactant-to-oil (S/O) ratio of 0.0307. At the end of the emulsion preparation cycle, the emulsion was sampled offline and online at various time intervals. The transmission spectra recorded at different sampling times were compared after normalization.[2,15] The changes in the normalized transmission spectra reflect, in this instance, changes in the droplet size distribution.[2,15] The shape of the transmission spectrum of the emulsion changed as a function of time. The emulsion was assumed to have reached stability once the spectral features remained constant. For the range of experimental conditions used, at approximately 2 h 15 min after decane addition, the shape of the spectrum remained constant, and this indicated that the stability of the emulsion had been achieved. Figure 3 shows typical changes in the observed normalized optical density (OD) at a wavelength of 252 nm as a function of time. After the emulsion achieves stability, the normalized OD at 252 nm remains unchanged as the time progresses. Figure 4 show a comparison of the normalized online and offline spectra after stability has been achieved. The spectra are undistinguishable once the emulsion has reached stability The distinct narrow peaks present in the higher wavelength region are known artifacts of the lamp and hence are disregarded during the deconvolution analysis of the measured spectra (see the next section). It is noteworthy that the mean diameter of the small-droplet populations remained fairly constant throughout the stabilization process, whereas the mean diameter of the large-particle populations and their corresponding mass fraction of oil changed significantly. Once the emulsion stabilizes, these values remain statistically constant along with the shape of the spectra.

TABLE II
Experimental Conditions

Experimental conditions	Temperature (°C)	pH	S/O
1	50	2	0.0154
2	60	2	0.0154
4	60	10	0.0154
5	50	2	0.046
6	60	2	0.046
7	22	10	0.046
8	60	10	0.046

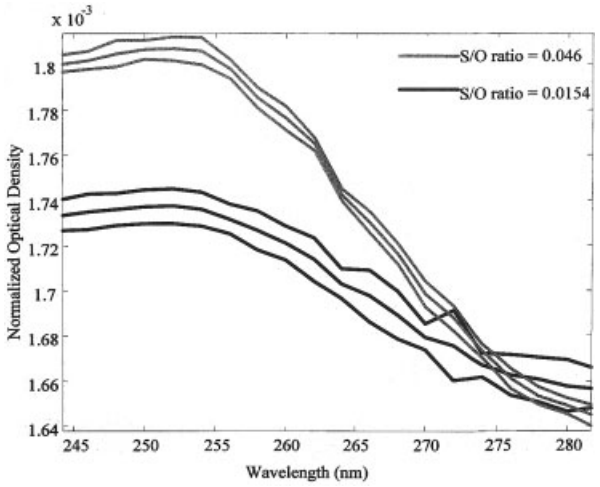

Figure 5 Comparison of the normalized mean OD spectra with the 95% confidence interval of a decane-in-PBS emulsion system at two different emulsifier concentrations at 50°C and pH 2 (amplified short wavelength region). The effect of the emulsifier concentration on the spectral features can be readily appreciated.

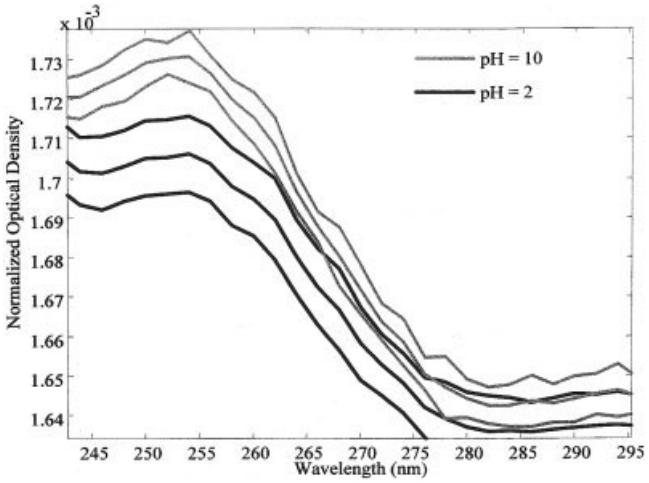

Figure 7 Comparison of the normalized mean OD spectra with the 95% confidence interval of a decane-in-PBS emulsion system at 60°C, with two different pH values, and with a low S/O ratio (0.0154; amplified short wavelength region). The effect of the pH on the spectral features can be readily appreciated.

Experimental reproducibility

Full replicate experiments performed at the center point confirmed that the total variance of the system was adequate for the discrimination of the main effects. In addition, three replicate measurements of the transmission spectra were obtained for the emulsion prepared at each of the conditions reported in Table II. The mean transmission spectrum and the 95% confidence intervals were calculated from the pooled variance estimates of all the replicates. The 95% confidence intervals reported herein reflect the measurement error, the sampling error, and the uncertainties introduced by temperature and flow fluctuations in the system. In Figures 5–9, the upper and lower bounds of the 95% confidence transmission spectra are reported along with mean transmission spectra. The spectral signals beyond the bounds of the confidence intervals are regarded as statistically different.

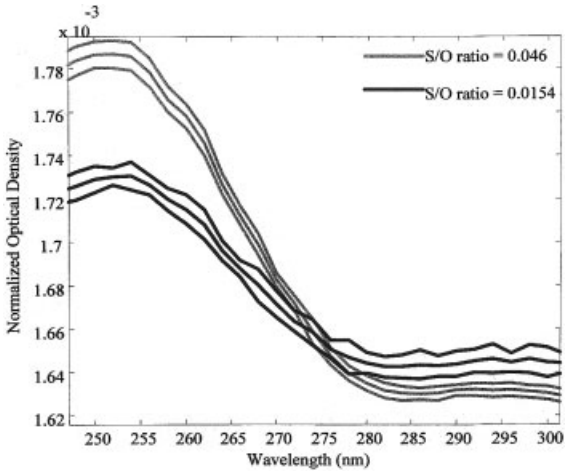

Figure 6 Comparison of the normalized mean OD spectra with the 95% confidence interval of a decane-in-PBS emulsion system at two different emulsifier concentrations at 60°C and pH 10 (amplified short wavelength region). The effect of the emulsifier concentration on the spectral features can be readily appreciated.

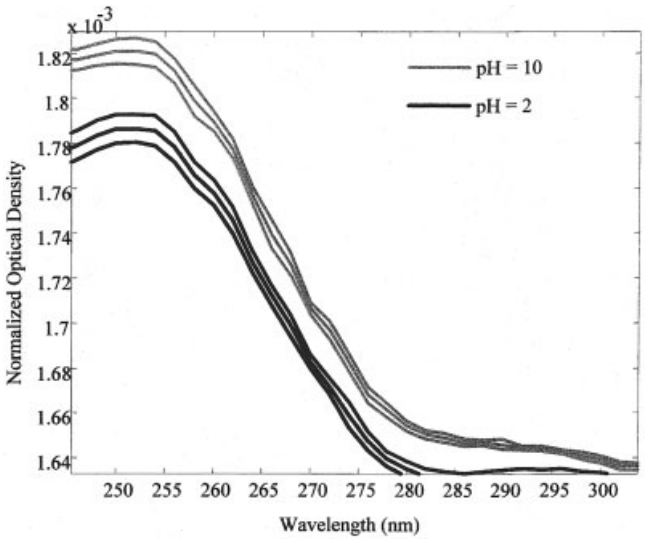

Figure 8 Comparison of the normalized mean OD spectra with the 95% confidence interval of a decane-in-PBS emulsion system at 60°C, with two different pH values, and with a high S/O ratio (0.046; amplified short wavelength region). The effect of the pH on the spectral features can be readily appreciated.

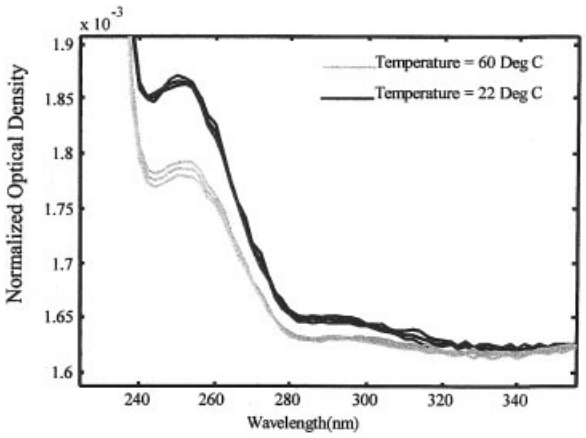

Figure 9 Comparison of the normalized mean OD spectra with the 95% confidence interval of a decane-in-PBS emulsion system at two temperatures, at pH 10, and with a high S/O ratio (amplified short wavelength region). The effect of the pH on the spectral features can be readily appreciated.

Optical properties

As indicated in part I of this study, the optical properties of the continuous phase [refractive index $n_0(\lambda_0)$] under the reaction conditions were estimated with the expression developed by Scheibener.[16] The optical properties of the styrene monomer were approximated from their measured absorption spectra and the Kramer–Kronigs transforms.[17,18] The optical properties of decane as functions of temperature were estimated with the Sellimeir–Drude equation.[3,19] The detailed procedures for calculating the optical properties are reported elsewhere.[14]

Spectral deconvolution

The emulsions were characterized in terms of the droplet size distribution, droplet number density, and droplet composition for each population in the dispersed phase. These parameters were obtained from the deconvolution of the measured transmission spectra for each set of experimental conditions with the interpretation model reported in part I of this series. The model was implemented within a standard Marquardt–Levenberg least-squares algorithm.[20] A mass-balance constraint on the oil concentration was applied as part of the optimization algorithm to resolve the spectra. Typically, the spectra were analyzed between 280 and 900 nm. This was done to minimize the effects of the unresolved absorption bands due to the emulsifier.

Experimental design

The experiments performed with the model emulsion systems were designed to explore the most important process variables known to affect the emulsification process. The selected process variables are the surfactant concentration, pH, and temperature. The aforementioned variables are expected to affect the emulsion characteristics, such as the stabilized interfacial area,[21] the composition of the dispersed phase,[22] and the size distribution of the discrete phase,[21,22] and as a result, the distributions of the nanodroplet and large-droplet populations.[21,22] The experiments were designed as a skewed factorial design with two levels and three variables with replicate experiments performed at the center point. Table II lists the different conditions under which the designed experiments were performed. The upper and lower levels of the S/O ratio were 0.046 and 0.0154, respectively. The upper level of the S/O ratio was almost 1.15 times that used in the standard recipe of emulsion polymerization experiments,[1,3] whereas the lower level was less than half the surfactant concentration of the standard recipe. In both instances, the surfactant concentration was higher than the critical micelle concentration. Therefore, the presence of micelles was expected in all cases. To verify the presence of micelles, experiments were performed with surfactant solutions at different concentrations, as described by Shastry.[14] The existence of a scattering component in the transmission spectra of the surfactant solutions under different conditions of the temperature, pH, and surfactant concentration strongly suggests the existence of micelles under these conditions.[14] The range of pH levels was decided on the basis of the dissociation characteristics of the surfactant; the pK_a value of the surfactant was estimated to be 6.91 ± 0.41.[14,23] Therefore, to span the range of protonated surfactant molecules to dissociated surfactant molecules, the lower pH level for the suspending medium was set at pH 2, and for the other end, pH 10 was selected.

The temperature levels were kept within the range typical of commercial emulsion polymerization processes. The higher and lower limits of the temperature were chosen to be 60 and 22°C. A skewed design with respect to the temperature was conducted to maximize the expected effects. Table II lists all the conditions under which the emulsions were prepared.

RESULTS AND DISCUSSION

As expected from the design of the experiments, the measured spectra of the emulsions and, therefore, the relative populations of nanodroplets and large droplets change dramatically as a result of the differences in the emulsification conditions. Figures 5–9 illustrate representative spectral differences in the transmission UV–vis spectra of the emulsions prepared under the emulsification conditions shown in Table II. Table III lists, qualitatively, the effects of changes in the manipulated variables on the characteristics of the droplet

TABLE III
Effects of the Manipulated Variables on the Mean Diameter (μ_s) and Standard Deviation (σ) of the Size Distribution and on the Weight Fraction of the Oil Phase (W_s) Contained in the Nanodroplet Population

Effect of pH			Effect of temperature				Effect of surfactant concentration			
At low surfactant concentration	At high surfactant concentration		At low surfactant concentration	At high surfactant concentration			At low pH		At high pH	
At high temperatures	At high temperatures	μ_s (N)	At high pH	μ_s (N_{PE})	At high pH	μ_s (N)	At high temperatures	$\mu s(D)$	At high temperatures	μ_s (D)
		σ (N)		σ (N_{PE})		σ (N)		σ (N)		σ (N)
		W_S (N)		W_S (N_{PE})		W_S (N)		W_S (I)		W_S (I)
At low temperatures	At low temperatures	μ_S (N_{PE})	At low pH	μ_S (N)	At low pH	μ_S (N)	At low temperatures	μ_S (D)	At low temperatures	μ_S (N_{PE})
		σ (N_{PE})		σ (N)		σ (N)		σ (N)		σ (N_{PE})
		W_S (N_{PE})		W_S (N)		W_S (N)		W_S (I)		W_S (N_{PE})

The direction of change for each set of conditions is indicated in parenthesis: I, increase; D, decrease; N, no change; N_{PE}, not possible to evaluate.

TABLE IV
Summary of the Experimental Results from the Deconvolution of the Spectra

Experimental conditions	D_S (nm)	σ_S	D_L (nm)	σ_L	W_S
Decane emulsions					
T = 50°C S/O = 0.0154 pH = 2	109	0.11	3409	0.59	18.0
T = 60°C S/O = 0.0154 pH = 2	106	0.15	3732	0.61	12.0
T = 60°C S/O = 0.0154 pH = 10	98	0.08	3613	0.62	16.2
T = 50°C S/O = 0.046 pH = 2	32	0.09	3449	0.59	76.5
T = 60°C S/O = 0.046 pH = 2	30	0.07	3773	0.6	79.9
T = 22°C S/O = 0.046 pH = 10	31	0.11	3660	0.57	77.2
T = 60°C S/O = 0.046 pH = 10	28	0.10	3575	0.59	80.6
Styrene emulsions					
T = 50°C S/O = 0.043 pH = 7	37	0.10	3246	0.20	36.8
Butyl methacrylate emulsions					
T = 60°C S/O = 0.043 pH = 7	38	0.10	3080	0.18	46.7

D_S = mean diameter of the nanodroplet population; D_L = mean diameter of the large droplet population; σ_S = standard deviation of the nanodroplet population; σ_L = standard droplet of the large population; W_S = weight fraction of the oil phase in the nanodroplet population; T = temperature.

populations. Table IV summarizes the quantitative deconvolution results for all experimental conditions.

Typical comparisons of measured and calculated spectra of the decane emulsions at the two extremes of the range of experimental conditions are shown in Figures 10 and 11. Details of the spectral deconvolution for all the experimental conditions are reported elsewhere.[14] The excellent agreement found between the measured and calculated spectra further supports the presence of at least two distinct droplet populations.

In addition to the deconvolution of the spectra, a theoretical analysis was conducted for each of the experimental points in the design to ascertain if the emulsifier concentration could support the surface area of the populations estimated from the spectroscopy measurements. The results of this analysis are tabulated in Table V.

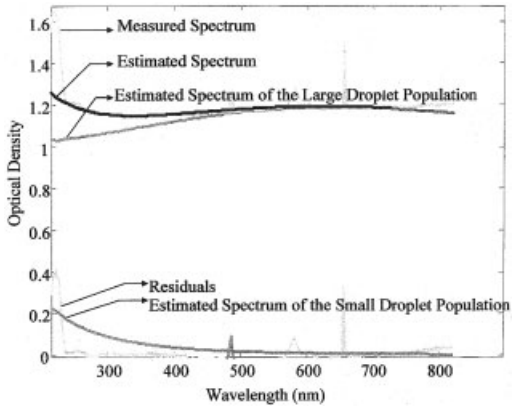

Figure 10 Deconvolution of the comparison of a measured transmission UV–vis spectrum of a decane-in-PBS emulsion (S/O = 0.0154, temperature = 50°C, and pH = 2). There is excellent agreement between the measured and calculated spectra as well as the spectral contributions of the large- and small-droplet populations. The residual spectrum shows the spectral features of the surfactant.

Effect of the surfactant concentration

As could be expected, the S/O concentration had a considerable effect on the size and concentration of the nanodroplet population. As the S/O ratio increased, the size of the nanodroplets varied from approximately 30 to 110 nm. The mean diameter of the small-particle populations at the high S/O ratio was around 30 nm, whereas at a low S/O ratio, the mean diameter was approximately 100–110 nm. Similarly, at low S/O ratios, only 18% of the dispersed phase was present in the small particles, whereas for the emulsion recipes with a higher S/O ratio, more than 70–80% of the dispersed phase appeared to be contained in the small-particle population.

Effect of the temperature

The effect of the temperature on the mean diameter and on the distribution of both droplet populations was small, regardless of the surfactant concentration or the pH. Although some differences could be observed in the spectra, these remained within the statistical variability of the experiments, and no definite conclusions can be drawn at this time.

Effect of the pH

The characteristics of the droplet populations also appear to be a weak function of pH over the pH range investigated; the size distributions and the relative concentrations of the populations present remained largely unaffected by the large changes in pH. As in the case of temperature, although some trends could be observed in the spectra, these remained within the statistical variability of the experiments, and therefore no definite conclusions could be drawn.

The effects of the emulsification conditions on the mean and standard deviation of the size distribution corresponding to the small-particle population and on the weight percentage of the oil phase contained in the small-particle population are qualitatively summarized in Table III.

Surfactant-stabilized area

The large mass fraction of the discrete phase contained in the nanodroplet population suggests a much larger surface area for stabilization than that anticipated from the traditional description of the emulsions before the addition of the initiator. It is therefore important to assess if the amount of emulsifier present can stabilize the surface area estimated from the spectroscopy measurements.

Under the assumption that the literature values for the surface area stabilized per molecule of emulsifier[1,24,25] are applicable, and with the spectroscopy-estimated surface area of the large-droplet population, a mass balance on the emulsifier yields the concentration of the emulsifier available to stabilize the surface area of the nanodroplet population.[14] If the total surface area of the nanodroplet population is divided by the concentration of the emulsifier available to stabilize it, the surface area stabilized per molecule of the emulsifier is obtained. As can be appreciated in Table V, these values (column 8) are in good agreement with the literature values[1] (column 7) for the emulsion recipes with low S/O ratios. For emulsions with high S/O (rows 4–7 in Table V), the area stabilized per molecule of the emulsifier increases dramatically as the size deceases and the fraction of the oil phase in the nanodroplet population increases. The increase in

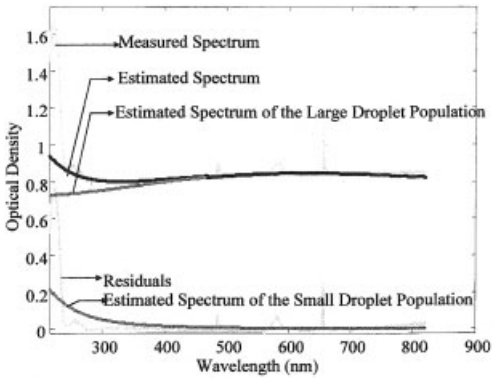

Figure 11 Deconvolution of the comparison of a measured transmission UV–vis spectrum of a decane-in-PBS emulsion (S/O = 0.046, temperature = 60°C, and pH = 10). There is excellent agreement between the measured and calculated spectra as well as the spectral contributions of the large- and small-droplet populations. The residual spectrum shows the spectral features of the surfactant.

TABLE V
Comparison of the Surfactant Distribution Between the Populations Identified in the Dispersed Phase

Experimental conditions	$A_T \times 10^{-5}$ (nm^2)	$A_S \times 10^{-5}$ (nm^2)	$A_L \times 10^{-5}$ (nm^2)	$[S]_L \times 10^7$ (g/mL)	$[S]_S \times 10^7$ (g/mL)	a_L (nm^2)	a_s (nm^2)	a_M at 10 nm	a_M at 3 nm
T = 50°C pH = 2 S/O = 0.0154	7.9	7.5	0.370	3.4	8.6	0.48	0.4	4.34	15.13
T = 60°C pH = 2 S/O = 0.0154	4.3	4.0	0.230	2.1	5.4	0.48	0.35	3	10.00
T = 60°C pH = 10 S/O = 0.0154	9.3	8.9	0.380	3.5	10	0.48	0.4	4.03	13.44
T = 50°C pH = 2 S/O = 0.046	344	344	0.330	3.0	82.5	0.48	1.88	6.18	20.66
T = 60°C pH = 2 S/O = 0.046	449	449	0.294	2.7	91.7	0.48	2.21	6.47	21.58
T = 22°C pH = 10 S/O = 0.046	435	434	0.402	3.7	100	0.48	1.94	6.26	20.88
T = 60°C pH = 10 S/O = 0.046	420	419	0.290	2.6	82.5	0.48	2.29	6.53	21.77

A_T, total surface area; A_S, surface area of the small droplet population; A_L, surface area of the large droplet population; $[S]_L$, grams of surfactant; per milliliter of emulsion used to stabilize the large droplet population; $[S]_S$, grams of surfactant per milliliter of emulsion used to stabilize the small droplet population; a_L, area stabilized per surfactant molecule for the large droplets; a_S, area stabilized per surfactant molecule for the nanodroplets; a_M, area stabilized per surfactant molecule for micelles (at the micellar diameters listed); T, temperature.

the stabilized area per emulsifier molecule is consistent with the expectation that the emulsifier efficiency increases with its concentration.[21] Furthermore, the emulsifier requirements to stabilize the nanodroplet populations are always smaller than the concentration required for the emulsification of the difference between the total oil concentration and the fraction of oil contained in large droplets. Because the known micellar sizes and the sizes of monomer-swollen micelles are much smaller than the sizes estimated for the nanodroplet populations, the surfactant concentration requirements are much higher for the same fraction of discrete phase. This can be clearly seen in Table V (columns 9 and 10), in which the required area for stabilization per molecule of surfactant is shown as a function of the micellar size. Clearly, the thermodynamic arguments favor the presence of nanodroplets. Therefore, it may be concluded that the presence of a nanodroplet population, with its concomitant large surface area, is feasible within the context of current theoretical values for the emulsifier efficiency.

CONCLUSIONS

This study has shown that the formulation of emulsions for emulsion polymerization reactions is likely to lead to the formation of two distinct droplet populations depending on the emulsification conditions: a previously unidentified population of nanodroplets ranging in size from 30 to 100 nm and a large-droplet population ranging in size from 1 to 5 μm. It has also been shown that a considerable fraction of the discrete phase is contained within the nanodroplet population, and this makes it a likely locus for particle nucleation. The identification of the droplet populations was made possible by the large dynamic range for particle analysis available through spectrophotometric measurements and by the use of model systems that not only mimic the dispersion behavior of monomers but also provide adequate contrast for the analysis.

The effects of emulsification conditions on the initial droplet populations have been experimentally and theoretically investigated with a dual objective: first, to provide further inferences and validation with respect to the presence of the nanodroplet populations, and second, to explore the main emulsification variables in a preliminary attempt to characterize the sensitivity of the discrete-phase distribution among the populations present. As a result, a preliminary experimental map of the behavior of the droplet populations has been drawn. Also, it has been shown, experimentally and in agreement with the theory, that the main variable controlling the discrete-phase distribution is the S/O ratio. Theoretical calculations based on accepted values for the area stabilized per molecule of surfactant further support the presence of the nanodroplet populations.

Clearly, additional studies on the spectroscopy behavior of labeled emulsifiers are necessary together with studies on both the emulsification of monomers and polymerization reactions conducted under the same set of conditions. These studies are underway, and their results will be published shortly.

The authors acknowledge the Particle Engineering Research Center at the University of Florida and its industrial partners ICI-Glidden, Lucent Technologies, and Xerox for their financial and technical support. The authors also acknowledge Carl Biver for reviewing this article.

References

1. Gilbert, R. G. In Emulsion Polymerization: A Mechanistic Approach; Academic: San Diego, 1995.
2. Shastry, V.; Garcia-Rubio, L. H. Handbook of Transport Data; Library of Physico-Chem Property Data; Gulf Publishing: Houston, 1995; p 45.
3. Celis, M. Ph.D. Dissertation, University of South Florida, 2000.
4. Yaws, C. L. Handbook of Transport Property Data; Library of Physico-Chem Property Data; Gulf Publishing: Houston, 1995; pp 45 and 49.
5. Dean, J. A. Handbook of Organic Chemistry; McGraw-Hill: 1987; Chapter 1, pp 136, 163, and 344.
6. Surface Tension Values of Common Test Liquids for Surface Energy Analysis, http://surface-tension.de/index.html (accessed September 2003).
7. Decane Material Safety, http://www.jtbaker.com/MSDS/englishhtml/d0136.htm (accessed September 2003).
8. Pure Component Properties, http://www.cheric.org/kdb/kdb/hcprop/showprop.php?cmpid=10 (accessed September 2003).
9. Safety Data Sheet for Styrene, http://www.petrochemistry.net/ftp/pressroom/CEFIC_20styrene_20SM_20SM_20MSDS_20V7_202005.doc (accessed December 2005).
10. MSDS Styrene, http://ptcl.chem.ox.ac.uk/MSDS/ST/Styrene.html (accessed September 2003).
11. Vara, J. M.S. Thesis, University of South Florida, 2000.
12. MSDS Butyl Methacrylate Monomer, http://physchem.ox.ac.uk/MSDS/BU/butyl_methacrylate_monomer.html (accessed September 2003).
13. Canadian Center for Occupational Health and Safety MSDS Methyl Methacrylate, http://www.intox.org/databank/documents/chemical/methymet/cie242.htm (accessed September 2003).
14. Shastry, V. Ph.D. Dissertation, University of South Florida, 2004.
15. Alupoei, C. M.S. Thesis, University of South Florida, 2001.
16. Scheibener, P.; Straub, J.; Levelt Songers, J. M. H.; Gallagher, J. S. J Phys Chem Ref Data 1990, 19, 677.
17. Kerker, M. The Scattering of Light and Other Electromagnetic Radiation; Pergamon: New York, 1969.
18. Bohren, C. F.; Huffman, D. R. Absorption and Scattering of Light by Small Particles; Wiley: 1983; pp 29, 80, 81, and 135.
19. Brooks, B. T.; Boord, C. E. The Chemistry of Petroleum Hydrocarbons; Reinhold: New York, 1983.
20. Marquadt Levenberg and Steepest Descent, http://duke.usask.ca/~merriam/inversion/CSEG7.pdf (accessed December 2005).
21. Research and Development of Surfactants, http://www.online-tensiometer.com/einsatz/f10_2.html#top (accessed September 2003).
22. Sherman, P. Emulsion Science; Academic: New York, 1968; Chapter 1.
23. Shastry, V.; MacDonald, S. ACD Laboratories, private communication.
24. Davies, J. T.; Rideal, E. K. Interfacial Phenomena; Academic: San Diego, 1961; p 232.
25. Drew, M. Surfaces, Interfaces and Colloids: Principles and Applications; VCH: Weinheim, 1991; p 227.